

Quantifying Bending Moments in Rail-Transit Concrete Sleepers

J. Riley Edwards, P.E., A.M.ASCE¹; Alvaro E. Canga Ruiz, S.M.ASCE²; Aaron A. Cook³; Marcus S. Dersch, P.E., A.M.ASCE⁴; and Yu Qian, Ph.D., A.M.ASCE⁵

Abstract: With use of concrete sleepers increasing for rail-transit applications in the United States, it is becoming more critical to quantify their revenue service flexural demands to improve sleeper design and maintenance practices. Rail-transit concrete sleeper bending moment field data were collected and processed to address topic areas relating to (1) overall field bending moment magnitude relative to design moments; (2) moment variation from sleeper to sleeper resulting from support conditions; and (3) seasonal variations in moments. Data from field locations on light and heavy rail-transit properties show levels of reserve flexural capacity (factors of safety) that reach as high as 6, significant sleeper-to-sleeper variability attributable to support conditions that can be as high as 100%, and seasonal variation in bending moments that is measurable but far lower than daily variability caused by temperature by a factor of 2. These data provide a valuable baseline for the future generation of mechanistic design standards for track infrastructure components. DOI: 10.1061/JTEPBS.0000125. © 2018 American Society of Civil Engineers.

Author keywords: Concrete sleeper; Field instrumentation; Rail transit; Light rail; Heavy rail; Flexural strength; Bending moments.

Background and Introduction

Ballasted track is the dominant type of track used for railway infrastructure throughout the world, and it typically consists of the rail, fastening systems, sleepers, ballast, subballast, and subgrade (Hay 1982). Currently in the United States, concrete is the second most common material used in the manufacture of sleepers, but concrete is the dominant sleeper material used in many other locations throughout the world (Railway Technology 2017; Van Dyk 2014). Because of the increased flexural strength, ductility, and resistance to cracking produced by pretensioned steel wires (Naaman 2004), prestressed concrete is the most common manufacturing method used to generate flexural rigidity to withstand the demanding loading environment imparted by passing trains. Additionally, prestressed concrete sleepers are commonly used in rail-transit applications because of their improved ability to maintain track gauge and the limited time that track is available for maintenance activities (McHenry and LoPresti 2016; Van Dyk 2014; Zeman 2010).

Although useful input data for the mechanistic design (Van Dyk et al. 2013) of concrete sleepers in heavy axle load (HAL) freight systems were documented in earlier research efforts (Edwards et al. 2017a), additional effort is required to generate a robust data set for rail-transit loads, bending moments, and displacements. At present, many design practices used for rail transit are borrowed from HAL freight railroad engineering; thus, the potential for incorrect and inefficient application of these standards exists. This potential inefficiency (i.e., overdesign) is being addressed through a research effort aimed specifically at rail-transit infrastructure funded by the Federal Transit Administration (FTA), with the objective of mechanistically designing track components based on actual field-loading conditions.

Most of the overly conservative designs have resulted in reasonable service lives to date, but future systems could be optimized to provide economies for new track construction and renewal activities. However, challenges can emerge from concrete sleepers that have been overdesigned with unnecessarily high levels of prestress, contributing to brittle failures (Windisch 1970). Additionally, striving for concrete with unnecessarily high levels of compressive strength could also contribute to premature brittle failures of sleepers (Gettu et al. 1990) and necessitate the use of premium (and more costly) mixture designs. Finally, prestress forces have been known to generate bursting stresses around wires or strands that leads to sleeper end cracking (Mayville et al. 2014), and reduction of these stresses would likely mitigate this type of bursting failure. Although the extent of the aforementioned concerns remains to be quantified, there is a clear economic benefit to designing and manufacturing sleepers that are optimally sized in terms of the cost savings for the component itself and the equipment needed to transport and install sleepers.

Although the design of prestressed precast monoblock sleepers has many different facets (e.g., including materials selection, economic impact, overall performance criteria, etc.), the flexural design is widely considered to be the most critical design element given its linkage to the structural integrity of the sleeper. Beyond quantifying bending moment magnitude, which could be incorporated into future mechanistic designs (Van Dyk et al. 2013),

¹Senior Lecturer and Research Scientist, Dept. of Civil and Environmental Engineering, Univ. of Illinois at Urbana-Champaign, 1243 Newmark Civil Engineering Laboratory, MC-250, 205 N. Mathews Ave., Urbana, IL 61801 (corresponding author). E-mail: jedward2@illinois.edu

²Graduate Engineer, Arup, 77 Water St., New York, NY 10005. E-mail: cangaru2@illinois.edu

³Engineering Associate, Union Pacific Railroad, 1400 Douglas St., Omaha, NE 68179. E-mail: aacook2@up.com

⁴Senior Research Engineer, Dept. of Civil and Environmental Engineering, Univ. of Illinois at Urbana-Champaign, 1240 Newmark Civil Engineering Laboratory, MC-250, 205 N. Mathews Ave., Urbana, IL 61801. E-mail: mdersch2@illinois.edu

⁵Assistant Professor, Dept. of Civil and Environmental Engineering, Univ. of South Carolina, 300 Main St.-C228, Columbia, SC 29208. E-mail: yuqian1@illinois.edu

Note. This manuscript was submitted on July 24, 2017; approved on September 13, 2017; published online on January 10, 2018. Discussion period open until June 10, 2018; separate discussions must be submitted for individual papers. This paper is part of the *Journal of Transportation Engineering, Part A: Systems*, © ASCE, ISSN 2473-2907.

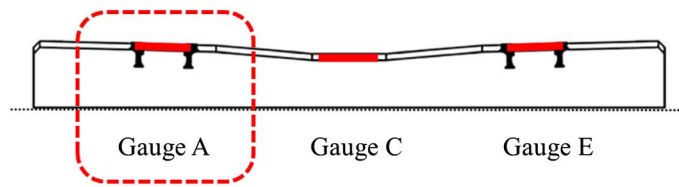


Fig. 1. Profile view of instrumented sleeper showing locations of strain gauges and example of rail seat with Gauge A installed

researchers and practitioners are interested in understanding the variability in flexural demands from sleeper to sleeper to aid in planning and prioritizing tamping operations. Additionally, variability in temperatures can impact bending moments in the field (Wolf et al. 2016), and the authors desire to quantify the seasonal variation in bending moments that can be expected on rail-transit systems. Flexural reserve capacity (i.e., ratio between sleeper design capacity and moment observed) and seasonal variability of moments have the potential for being more pronounced in the rail-transit loading environment because of the ratio between the average wheel loads and flexural resistance of sleepers being lower than those seen in the HAL freight environment. In other words, seasonal and other sources of variation that are independent of load may be more critical in rail-transit applications than those observed in HAL freight service (Wolf 2015; Wolf et al. 2016) because of the distinctly different loading magnitudes yet similar sectional moduli of the sleepers.

To address the aforementioned topic areas of sleeper flexural reserve capacity quantification, sleeper-to-sleeper variability, and seasonal variation of moments, concrete surface strain-gauge instrumentation was deployed in the field on both light and heavy rail-transit systems. This method was previously developed, deployed, and validated by the University of Illinois at Urbana-Champaign (UIUC) and has proven useful in answering similar questions for HAL freight applications (Edwards et al. 2017b).

Methodology

Instrumentation Technology: Concrete Surface Strain Gauges

Researchers have previously undertaken projects using either embedded or surface strain gauges to quantify field bending moments of concrete sleepers (Edwards et al. 2017a; Kerokoski et al. 2016; Mayville et al. 2014; Venuti 1990, 1970), which were summarized by Edwards et al. (2017b).

Building on these prior experiences, UIUC researchers developed a holistic plan to instrument sleepers and collect reliable bending moment data, which was described by Edwards et al. (2017b). Using this methodology, data from strain gauges were collected using a National Instruments (NI) compact data acquisition system (cDAQ) (Austin, Texas) (National Instruments 2017; Wolf 2015). The instrumentation deployed was also designed to be temperature-compensating to minimize error caused by temperature fluctuations from direct sunlight, shading from passing trains, and seasonal climate conditions. cDAQ signals from the instrumentation were recorded through a NI LabVIEW virtual instrument (VI) (Austin, Texas).

A minimum sampling rate was determined based on the maximum authorized train speed at each field experimentation location

and the desired data sampling resolution, where the sampling resolution is the distance the train travels between consecutive samples. The sampling resolution desired for the example application discussed in this paper was 12.7 mm (0.5 in.). Based on these requirements, prior experience, and expert recommendation, the sampling rate was set as 2,000 Hz.

Instrumentation Deployment on Sleeper

Bending strains at critical discrete locations along the length of the sleeper were measured to quantify the flexural behavior of the sleeper under revenue service train loading. As such, concrete surface strain gauges were oriented longitudinally along the chamfer near the top surface of the sleeper. Three strain gauges (labeled A, C, and E) were used on each sleeper, with one applied at each of the two rail seats and one at the center (Fig. 1). Additional relevant dimensions and properties for the two types of rail-transit sleepers investigated in this paper are provided in Table 1, which also include a typical sleeper used in HAL freight service. All three types of sleepers in Table 1 use a prestressing tendon that is 5.32 mm (0.209 in.) in diameter and use similar concrete mixture designs. Specification design capacities in Table 1 refer to the end-user (transit agency or railroad) value that is required to be met or exceeded for flexural strength, and design values are the capacities that are associated with the unique sleeper designs that are supplied by the sleeper manufacturers.

The process of instrumenting sleepers in the field, including the protection of strain gauges, is shown in Fig. 2 and was described in greater detail by Edwards et al. (2017b). To relate the field-measured strains to a bending moment, calibration factors were generated through laboratory experimentation, as described in the next section.

Laboratory Sleeper Moment Calibration

Laboratory calibration was conducted using the static tie tester (STT) (Fig. 3) at UIUC's Research and Innovation Laboratory (RAIL) in the Harry Schnabel, Jr. Geotechnical Engineering Laboratory in Champaign, Illinois. The STT can apply known loads to test the flexural and/or compressive behavior of concrete sleepers. A calibrated load cell is used to monitor the applied loads to relate strain and bending moments.

Calibration of surface strain gauges requires multiple (minimum of three) sleepers of the same design, concrete compressive strength, and approximate age to generate representative calibration factors. Laboratory calibration included rail seat positive and negative bending tests and sleeper center positive and negative bending tests. Moments were applied by loading the sleeper using preestablished standardized testing procedures outlined in the American Railway Engineering and Maintenance-of-Way Association (AREMA) *Manual for railway engineering* (AREMA 2016). Detailed calibration processes and procedures, including equations

Table 1. Characteristics of Two Types of Sleeper Used in This Study for Light and Heavy Rail Applications, and Comparison with a Typical HAL Freight Sleeper

Sleeper	Characteristic	Specification/design	MetroLink		NYCTA		HAL freight	
			SI	Imperial	SI	Imperial	SI	Imperial
Static wheel loads	Maximum (AW3)	—	41.8–55.6 kN	9.4–12.5 kips	62.9 kN	14.1 kips	35.8 kips	159 kN
	Minimum (AW0)	—	28.9–42.7 kN	6.5–9.6 kips	50.6 kN	11.4 kips	Varies	Varies
Sleeper geometry	Length	—	2.51 m	8 ft 3 in.	2.59 m	8 ft 6 in.	2.59 m	8 ft 6 in.
	Tie spacing	—	0.76 m	30 in.	0.61 m	24 in.	0.61 m	24 in.
Sleeper prestressing	Number of tendons	—	12		18		20	
	Jacking force	—	31.1 kN	7 kips	31.1 kN	7 kips	31.1 kN	7 kips
	Precompression (sleeper center)	—	10,204 kN/m ²	1.48 ksi	13,858 kN/m ²	2.01 ksi	15,444 kN/m ²	2.24 ksi
Sleeper design capacity	Center negative	Specification	16.3 kN · m	144 kip · in.	19.0 kN · m	168 kip · in.	26.0 kN · m	230 kip · in.
		Design	16.6 kN · m	147 kip · in.	21.9 kN · m	194 kip · in.	26.0 kN · m	230 kip · in.
	Center positive	Specification	10.5 kN · m	93 kip · in.	13.3 kN · m	118 kip · in.	—	—
		Design	16.3 kN · m	105 kip · in.	14.9 kN · m	132 kip · in.	21.0 kN · m	186 kip · in.
	Rail seat positive	Specification	20.2 kN · m	179 kip · in.	28.3 kN · m	250 kip · in.	33.9 kN · m	300 kip · in.
		Design	25.0 kN · m	221 kip · in.	32.0 kN · m	283 kip · in.	43.1 kN · m	381 kip · in.
	Rail seat negative	Specification	12.0 kN · m	106 kip · in.	15.6 kN · m	138 kip · in.	—	—
		Design	15.4 kN · m	136 kip · in.	20.1 kN · m	178 kip · in.	24.7 kN · m	219 kip · in.

**Fig. 2.** (a) Sleepers being instrumented with concrete surface strain gauges; (b) completed St. Louis MetroLink light-rail field experimentation location**Fig. 3.** Static tie tester at UIUC used for laboratory calibration of concrete sleepers

to relate laboratory load and strain to field data, have been detailed by Wolf (2015) and Edwards et al. (2017b).

Field Deployment

Between 2015 and 2017, seven field deployments using this surface strain-gauging technology have been installed by UIUC researchers throughout the United States to answer a variety of questions that require quantification of field concrete sleeper bending moments. The specific field experimentation discussed in this paper was conducted on two ballasted track rail-transit systems, St. Louis MetroLink at East St. Louis, Illinois (hereafter referred to as MetroLink) and MTA New York City Transit Authority (NYCTA) at Far Rockaway, New York, (hereafter referred to as NYCTA). Because of the observed variability in support conditions seen in past field experimentation (Edwards et al. 2017a; Gao et al. 2016; Wolf 2015), instrumentation was placed on five consecutive sleepers at each field test location (Fig. 4). Additionally, five sleepers were selected based on the widely accepted theory on the distribution of vertical load to five consecutive sleepers (Hay 1982;

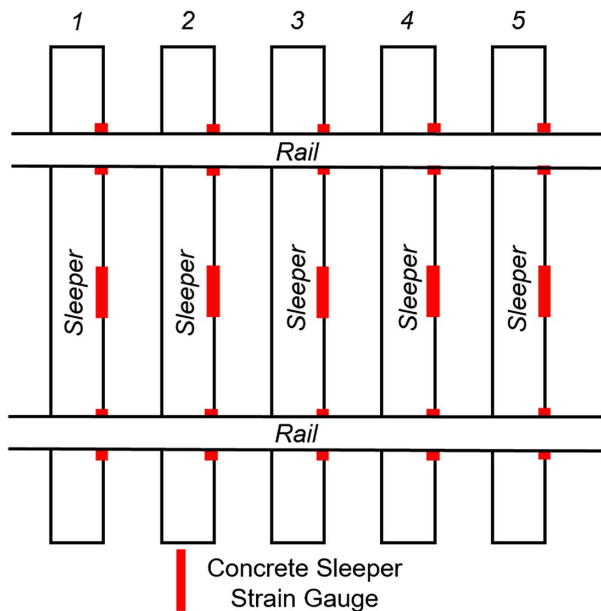


Fig. 4. Field experimentation site layout with five sleepers showing locations of the used concrete surface strain gauges

Van Dyk 2014) and with the aim of collecting replicate data to provide insight into the variability of support conditions.

Data Analysis Procedure

To quantify the bending moments that concrete sleepers experience in revenue service, peaks in the strain-gauge signal caused by sleeper bending attributable to a wheel or axle load must be extracted from the data stream collected at 2,000 Hz. This was accomplished using a modified version of the findpeaks function in *MATLAB*. To improve the performance of this function for this application, several of the built-in options were used, and additional modifications were made to the code that was originally developed by Wolf (2015).

Before the peaks were obtained, the strain signal was zeroed using data captured before the arrival of the first axle, and a linear baseline correction was applied to adjust for any signal drift over the course of a single train pass. As such, data collection was initiated several seconds prior to the arrival of the leading axle to provide a stable zero point for the sleeper under no applied load. Additionally, the data collection was ended several seconds after the final train axle passed to serve as an end point for the baseline correction. To ensure that the true peaks were being captured by the program, as opposed to false peaks that did not represent the extreme strain reading for a given axle pass, a minimum spacing between the peaks was specified and a minimum value for all peaks was set. A low-pass filter was developed and used for the processing of the strain field data. Additional detail on filtering and processing of data was previously documented by Edwards et al. (2017b).

Fig. 5 (left vertical axis) shows an example of a typical strain-gauge signal for a center gauge for a single MetroLink train pass made up of two six-axle light-rail vehicles (LRVs). The signal was zeroed out and the peaks were numbered in sequence, which were then converted into bending moments using the laboratory moment calibration factors described previously (Fig. 5, right vertical axis).

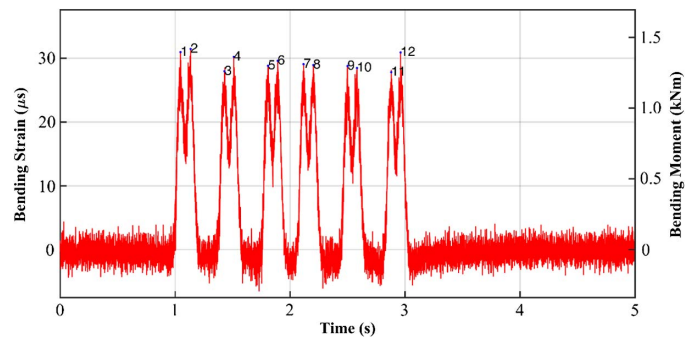


Fig. 5. Typical sleeper center strain signal and resulting center bending moment captured under the passage of a 12-axle St. Louis MetroLink light-rail trainset

Results

The instrumentation plan described in this paper was deployed for approximately 1 year on each of the two rail-transit properties. In total, 27,092 light-rail train passes were captured by the MetroLink site from March 18, 2016, until May 19, 2017, and another 11,597 heavy-rail train passes were captured by the NYCTA site between April 26, 2016, and February 27, 2017. For the duration of these deployments, the instrumentation plan described in this paper proved to be robust. Other field sites have experienced similar successes in terms of instrumentation robustness (Edwards et al. 2017b). Using these data from MetroLink and NYCTA, UIUC researchers analyzed the bending moments induced by loaded axles from the signals of the center and rail seat strain gauges (Gauges A, C, and E).

Magnitude of Bending Moments and Comparison to Standards and Design Capacities

The concrete sleeper center negative (C-) bending moment percent exceeding distribution for the aforementioned trains are shown in Fig. 6, which shows both the overall magnitude and variability of moments. It is evident that the variability and range associated with NYCTA moments exceed that of MetroLink, as evidenced by the shallower slope of the NYCTA data. Additionally, similar plots are shown for the rail seat positive bending moments in Fig. 7, with greater variability and range seen in the NYCTA data. These distributions are also shown in comparison to the specifications and

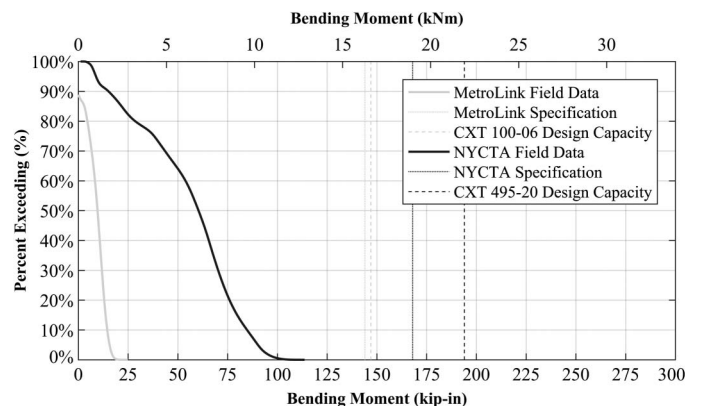


Fig. 6. Distribution of MetroLink and NYCTA C- bending moments for each axle and comparison with design capacity and transit property specifications

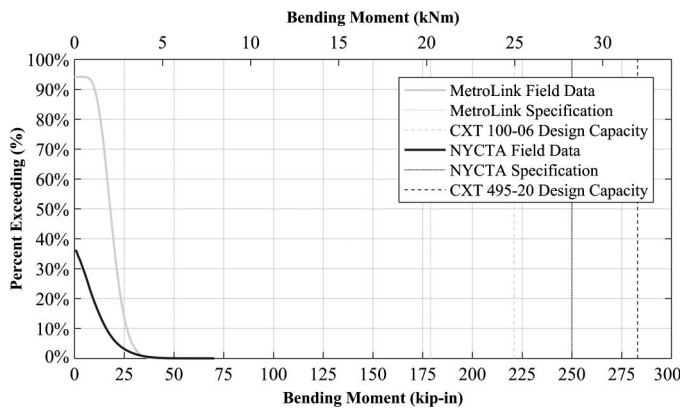


Fig. 7. Distribution of MetroLink and NYCTA RS+ bending moments for each axle and comparison with design capacity and transit property specifications

design capacities for both rail seat positive and center negative cracking, which are most commonly based on limits generated using AREMA recommended design practices (AREMA 2016). These values, generated using AREMA (2016), define a threshold that a bending moment that would need to exceed before a crack propagates to the first level of prestress.

None of the sleeper bending moments recorded reached the specification or design limit shown with vertical lines (Figs. 6 and 7). This is especially evident at the rail seats because the 95th percentile rail seat positive (RS+) moment values were less than 10% of the 20.2 kN · m (179 kip · in.) and 28.2 kN · m (250 kip · in.) specification limits for sleeper flexural design for MetroLink and NYCTA, respectively. When combined with high estimates for input wheel loads in design specifications, AREMA recommendations can significantly overestimate the flexural demand at the sleeper rail seat (Fig. 7). Compared with RS+ moments, 95th percentile C− bending moments were closer to the specification values, reaching as much as 50% of the 16.3 kN · m (144 kip · in.) and 19.0 kN · m (168 kip · in.) values for MetroLink and NYCTA, respectively. This indicates that center bending conditions may govern the design in terms of factors of safety (AREMA 2016) (Fig. 6). This finding is also in agreement with a previous survey of industry experts, which suggested that center cracking of concrete sleepers was more commonly seen in the field, albeit in HAL freight railroad applications (Van Dyk 2014). This type of failure may be preferable to infrastructure owners given it is more easily detected through visual inspection.

Additionally, when dividing the design capacity of the sleeper at the center or rail seat by the observed field moments at varying percentiles, a measure of reserve capacity is generated (Table 2). Current sleeper designs, even when compared with the maximum bending moments experienced in the field, have a reserve capacity exceeding 3.2 in RS+ bending for MetroLink and exceeding 1.7 in C− bending for NYCTA. These respective reserve capacity factors further increase to 7.6 and 2.1 when considering 95th percentile bending moments.

Reserve design capacities are consistently higher for MetroLink than NYCTA. There are a variety of factors that could influence this including the sleeper design and its related assumptions, the input rail seat loads (largely a function of wheel health/maintenance) and the sleeper support conditions (largely a function of track health/maintenance).

Of additional interest is the fact that positive center moments were captured on MetroLink and negative rail seat moments were captured on NYCTA, hence the negative values of reserve design

Table 2. Sleeper Reserve Capacity for Light-Rail (MetroLink) and Heavy-Rail (NYCTA) Transit

Percentile bending moment	Light rail		Heavy rail	
	Center	Rail seat	Center	Rail seat
Minimum	−4.92	−3.43	168.52	−2.71
0.1%	−7.79	−5.86	49.40	−4.92
1%	−9.79	−8.06	32.15	−6.12
5%	−18.29	−14.71	21.89	−7.57
10%	−95.87	21.69	12.81	−8.75
90%	10.11	8.38	2.29	17.76
95%	9.36	7.63	2.15	13.18
99%	8.35	6.54	1.98	8.61
99.9%	7.52	5.67	1.86	6.34
Maximum	5.90	3.21	1.71	4.03

Note: Reserve design capacity = (Design capacity)/(Measured bending moment).

capacity, indicating that the opposite moment was recorded (e.g., rail seat negative and center positive). Although these values are not often expected under field loading conditions, they do occur, and this paper's data provide insight regarding the frequency of these moments, which are not always considered in design specifications. It is interesting that the lowest reserve capacity ratios are found for RS− as opposed to RS+ for NYCTA and for C+ as opposed to C− for MetroLink. These apparent contradictions of conventional wisdom are attributable to the specific support conditions that were present, with the MetroLink sleepers being well-supported at the rail seat and NYCTA sleepers having more support at the center, as evidenced by the high C− bending moments. Furthermore, this finding can provide a method for future estimation of support conditions and process to infer whether center binding is present.

Sleeper-to-Sleeper Moment Variability

A critical question that researchers are desirous of addressing is what the degree of variability exists among bending moments collected from consecutive sleepers. This question has been addressed in earlier researches aimed primary at the HAL freight environment (Edwards et al. 2017b), but no work to date has been aimed at rail-transit concrete sleepers and operating conditions. Figs. 8 and 9 show the distribution of C− and RS+ bending moments, respectively, under MetroLink light rail–transit loading for the seven sleepers and 14 rail seats. Figs. 10 and 11 show the same distributions under heavy-rail traffic on NYCTA.

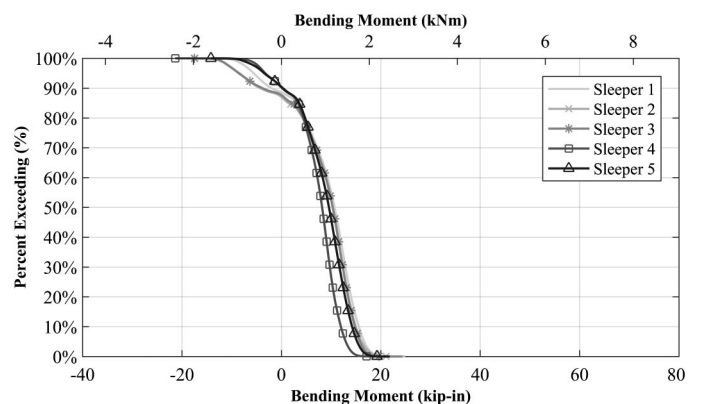


Fig. 8. Distributions showing sleeper-to-sleeper variability of C− bending moments for light rail–transit loading on St. Louis MetroLink

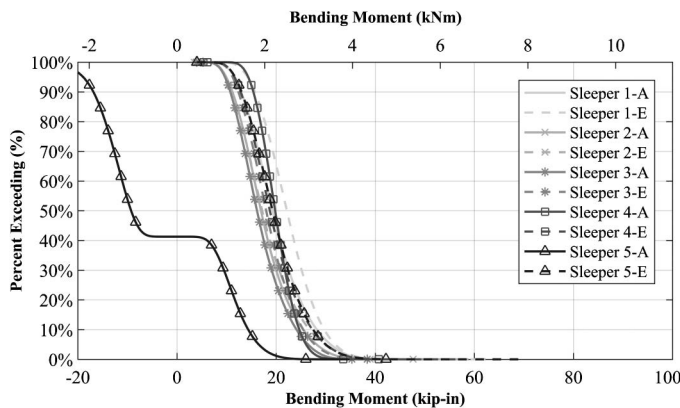


Fig. 9. Distributions showing sleeper-to-sleeper variability of RS+ bending moments for light rail-transit loading on St. Louis MetroLink

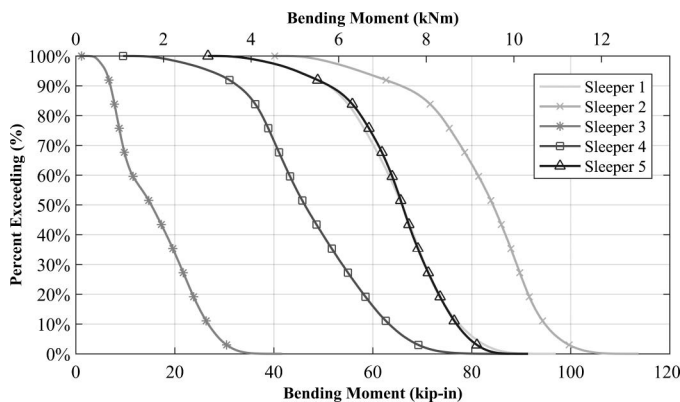


Fig. 10. Distributions showing sleeper-to-sleeper variability of C- bending moments for heavy rail-transit loading on NYCTA

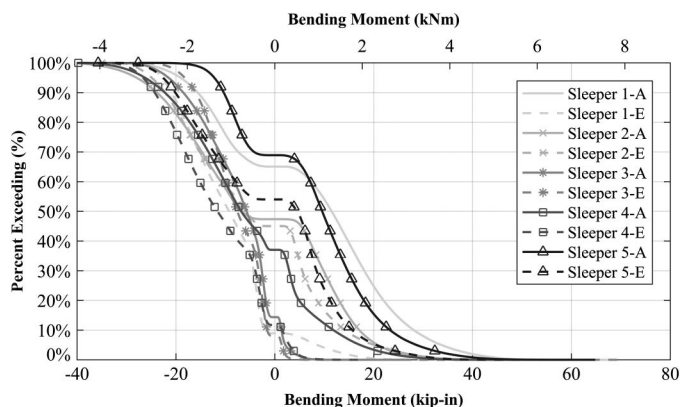


Fig. 11. Distributions showing sleeper-to-sleeper variability of RS+ bending moments for heavy rail-transit loading on NYCTA

With the exception of one rail seat's bending moment distribution (Sleeper 5-A), the sleeper-to-sleeper variability of the bending moments experienced on MetroLink was as low as 10%. The variability of the bending moments at both the rail seat (RS+) and sleeper center (C-) are considerably higher at NYCTA, reaching as high as 100%. This range in variabilities may be caused by, in

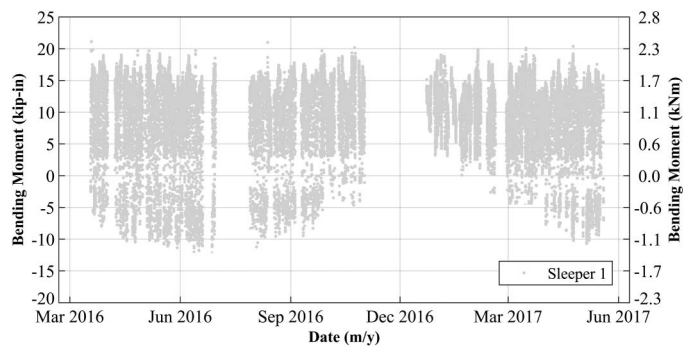


Fig. 12. Distributions showing seasonal variation of C- bending moments for light rail-transit loading on St. Louis MetroLink

part, different support conditions that are generated by unique track deterioration rates attributable to static railcar axle loads on NYCTA, which are approximately twice the magnitude of MetroLink. Additionally, not only are the wheel loads lower on MetroLink, but the line is of newer construction dating to 2003 and has required little (if any) tamping activities since construction.

For both sites and rail-transit modes, it is evident that there is higher variability among the RS+ bending moments than the C- moments. This is likely attributable to the fact that the rail seat moments are the first location in which wheel loads are accepted by the sleeper and are apt to encounter irregularities in wheel health and dynamic loading conditions that are less pronounced at the sleeper center (Wolf 2015).

Seasonal Effect on Bending Moments

Temperature-induced curl of the sleeper attributable to varied temperatures on the top and bottom (i.e., temperature gradient) has been shown to impact the flexural demand placed on the sleeper (Wolf et al. 2016). Initially, curl was found to change over the course of the day as the temperature gradient changed, which was found in both laboratory and field settings (Wolf 2015). Temperature gradients were also found to fluctuate over the course of the year under HAL freight operations, and these changes affected the bending moments induced in the concrete sleepers (Wolf 2015; Wolf et al. 2016), a behavior similar to that which has been noted in rigid-pavement applications (Beckemeyer et al. 2002).

For the rail-transit domain, Fig. 12 shows the seasonal variation of bending moments throughout a year of data collection at MetroLink, with single data points representing the average of a train pass over the site. Fig. 13 shows similar data for NYCTA. These data represent only one sleeper at each field testing location for graphical clarity, but the sleeper selected was indicative of the overall behavior observed at each site.

Seasonal variation is further demonstrated by extracting the daily average for each for each of the center gauges on the two rail-transit systems, shown in Figs. 14 and 15 for MetroLink and NYCTA, respectively. The variation in absolute bending moment values seen in Fig. 15 maps to the variability that was seen at the NYCTA field site as discussed in earlier.

The daily average train pass fluctuations in bending moments ranged by as much as $3.3 \text{ kN} \cdot \text{m}$ ($30 \text{ kip} \cdot \text{in.}$) and $4.5 \text{ kN} \cdot \text{m}$ ($40 \text{ kip} \cdot \text{in.}$) for MetroLink and NYCTA, respectively. Based on results from the two field sites with their specific support conditions, the daily fluctuations in C- bending moments caused by temperature exceed the seasonal variability by a factor of approximately 2.

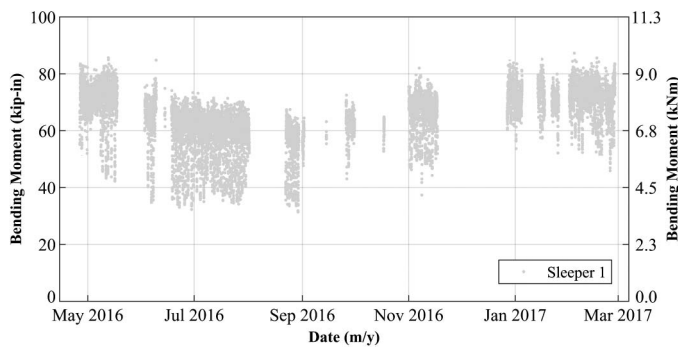


Fig. 13. Distributions showing seasonal variation of C- bending moments for heavy rail-transit loading on NYCTA

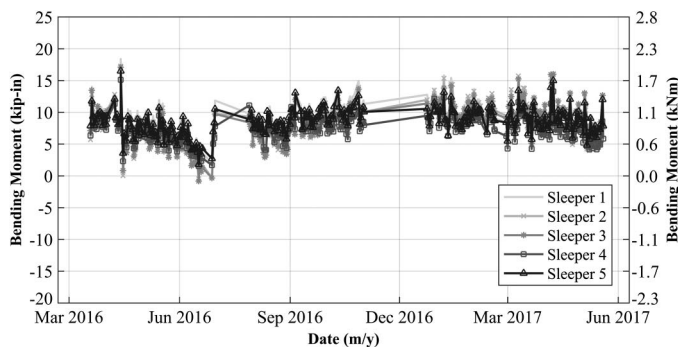


Fig. 14. Distributions showing sleeper-to-sleeper variability of average train pass C- bending moments for light rail-transit loading on MetroLink

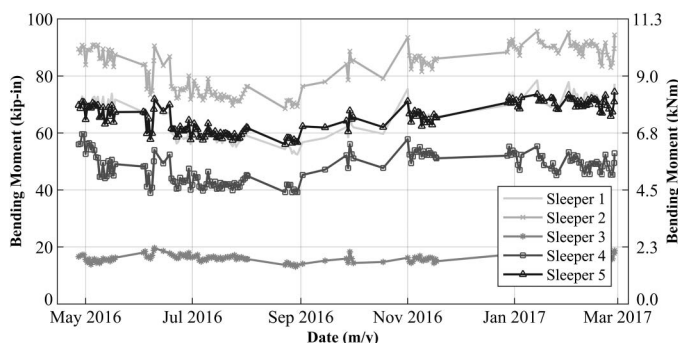


Fig. 15. Distributions showing seasonal variation of average train pass C- bending moments for heavy rail-transit loading on NYCTA

Figs. 14 and 15 also demonstrate a clear seasonal trend, with higher absolute center negative bending moments being applied during the winter months because of the widely-accepted theory of the track being stiffer during cold weathers (Cai et al. 1994). Additionally, although not investigated in this phase of research, the authors acknowledge deterioration as another factor that could impact the long-term flexural behavior of sleepers.

Conclusions

This concrete surface strain-gauge instrumentation methodology and deployment was successful in measuring bending strains and

resulting moments experienced by a two rail-transit modes in the United States. Through field deployments on MetroLink (light rail) and NYCTA (heavy rail), the following questions were addressed to aid in the future mechanistic design of concrete sleepers for rail-transit applications:

- What is the magnitude of flexural demands placed on sleepers, and how do these compare to specifications and standards in terms of residual capacity? The magnitude of maximum center negative bending moments ranged from 2.8 kN · m (25 kip · in.) on MetroLink (light rail) to 13.5 kN · m (120 kip · in.) on NYCTA (heavy rail). Significant residual capacity was found, and considering the 99% percentile bending moments, residual load factors of approximately 6 and 2 were found for light and heavy rail-transit systems, respectively;
- Do the bending moments experienced by concrete sleepers on rail-transit systems vary from sleeper to sleeper? Yes, ranging from as little as 10% for C- bending on MetroLink to as much as 100% on NYCTA. This is a similar finding to that previously demonstrated in the HAL freight loading environment. Sleeper-to-sleeper variability between the two transit modes was also quite different, with the greatest variability associated with center negative bending moments found on NYCTA, which experienced higher loads and differing maintenance practices; and
- Do seasonal effects have an influence on the flexural demands of concrete sleepers? Seasonal effects were observed, but these effects were found to be overshadowed by daily fluctuations in bending moments caused by temperature-induced curl in the sleeper by a factor of 2. This phenomenon seemed to be similar, but more pronounced, than earlier findings from HAL freight railroad instrumentation deployments.

Acknowledgments

This research is primarily funded by the United States Department of Transportation (USDOT) Federal Transit Administration (FTA). The published material in this report represents the position of the authors and not necessarily that of the DOT. Access to rail-transit infrastructure for testing was provided by St. Louis MetroLink, MTA New York City Transit Authority (NYCTA), and Union Pacific Railroad (operator of Metra's UP West Line in Chicago), and the authors are grateful for the tremendous support provided by all three organizations. The authors would also like to thank Matt Csenge and Xiao (Sean) Lin for their assistance in conducting field instrumentation. J. Riley Edwards has been supported in part by grants to the UIUC Rail Transportation and Engineering Center (RailTEC) from CN and Hanson Professional Services.

References

- AREMA (American Railway Engineering and Maintenance-of-Way Association). (2016). *Manual on railway engineering*, Landover, MD.
- Beckemeyer, C., Khazanovich, L., and Thomas Yu, H. (2002). "Determining amount of built-in curling in jointed plain concrete pavement: Case study of Pennsylvania I-80." *Transp. Res. Rec.*, 1809, 85–92.
- Cai, Z., Raymond, G. P., and Bathurst, R. J. (1994). "Estimate of static track modulus using elastic foundation models." *Transp. Res. Rec.*, 1470, 65.
- Edwards, J. R., Dersch, M. S., and Kernes, R. G. (2017a). "Improved concrete crosstie and fastening systems for US high speed passenger rail and joint corridors." *Final Rep. DOT/FRA/ORD-17/23*, Federal Railroad Administration, Washington, DC, 58.
- Edwards, J. R., Gao, Z., Wolf, H. E., Dersch, M. S., and Qian, Y. (2017b). "Quantification of concrete railway sleeper bending moments using surface strain gauges." *Measurement*, 111, 197–207.

- Gao, Z., Wolf, H. E., Dersch, M. S., Qian, Y., and Edwards, J. R. (2016). "Field measurements and proposed analysis of concrete cross-tie bending moments." *Proc., American Railway Engineering and Maintenance of Way Association Annual Meeting*, Orlando, FL.
- Gettu, R., Bazant, Z. P., and Karr, M. E. (1990). "Fracture properties and brittleness of high-strength concrete." *ACI Mater. J.*, 87(6), 608–618.
- Hay, W. W. (1982). *Railroad engineering*, 2nd Ed., Wiley, New York.
- Kerokoski, O., Rantala, T., and Nurmikolu, A. (2016). "Deterioration mechanisms and life cycle of concrete monoblock railway sleepers in Finnish conditions." *World Congress on Railway Research*, Milan, Italy.
- MATLAB [Computer software]. MathWorks, Natick, MA.
- Mayville, R. A., Jiang, L., and Sherman, M. (2014). *Performance evaluation of concrete railroad ties on the Northeast corridor*, Federal Railroad Administration, Washington, DC.
- McHenry, M., and LoPresti, J. (2016). "Field evaluation of sleeper and fastener designs for freight operations." *World Congress on Railway Research*, Milan, Italy.
- Naaman, A. E. (2004). *Prestressed concrete analysis and design: Fundamentals*, 2nd Ed., Techno, Ann Arbor, MI.
- National Instruments. (2017). "CompactDAQ." Austin, TX.
- Railway Technology. (2017). "At a glance: Railway sleeper materials." (<http://www.railway-technology.com/features/feature92105/>) (Jul. 20, 2017).
- Van Dyk, B. J. (2014). "Characterization of the loading environment for shared-use railway superstructure in North America." M.S. thesis, Univ. of Illinois at Urbana-Champaign, Champaign, IL.
- Van Dyk, B. J., Edwards, J. R., Ruppert, C. J., Jr., and Barkan, C. P. (2013). "Considerations for mechanistic design of concrete sleepers and elastic fastening systems in North America." *Proc., 2013 Int. Heavy Haul Association Conf.*, International Heavy Haul Association, Virginia Beach, VA, 4.
- Venuti, W. (1970). *Field investigation of the Gerwick RT-7 prestress concrete tie*, San Jose State Univ., San Jose, CA.
- Venuti, W. (1990). *Report on the structural response of the BART concrete ties*, San Jose State Univ., San Jose, CA.
- Windisch, A. (1970). "Safety to brittle failure in prestressed concrete structures with bond." *Period. Polytech. Civ. Eng.*, 14(4), 1–341.
- Wolf, H. E. (2015). "Flexural behavior of prestressed concrete monoblock cross-ties." M.S. thesis, Univ. of Illinois at Urbana-Champaign, Champaign, IL.
- Wolf, H. E., Qian, Y., Edwards, J. R., Dersch, M. S., and Lange, D. A. (2016). "Temperature-induced curl behavior of prestressed concrete and its effect on railroad cross-ties." *Constr. Build. Mater.*, 115, 319–326.
- Zeman, J. C. (2010). "Hydraulic mechanisms of concrete-tie rail seat deterioration." M.S. thesis, Univ. of Illinois at Urbana-Champaign, Champaign, IL.